



# Comprehensive assessment of dissolved organic matter processing in the Amazon River and its major tributaries revealed by positive and negative electro-spray mass spectrometry and NMR spectroscopy



Siyu Li <sup>a</sup>, Mourad Harir <sup>a,b</sup>, Philippe Schmitt-Kopplin <sup>a,b</sup>, Michael Gonsior <sup>c</sup>, Alex Enrich-Prast <sup>d,e</sup>, David Bastviken <sup>d</sup>, Juliana Valle <sup>a</sup>, Fausto Machado-Silva <sup>f,g</sup>, Norbert Hertkorn <sup>a,\*</sup>

<sup>a</sup> Research Unit Analytical Biogeochemistry, Helmholtz Munich, Ingolstaedter Landstrasse 1, 85764 Neuherberg, Germany

<sup>b</sup> Chair of Analytical Food Chemistry, Technische Universität München, Alte Akademie 10, 85354 Freising-Weihenstephan, Germany

<sup>c</sup> University of Maryland Center for Environmental Science, Chesapeake Biological Laboratory, 146 Williams Street, Solomons, MD 20688, United States

<sup>d</sup> Department of Thematic Studies – Environmental Change, Linköping University, SE-581 83 Linköping, Sweden

<sup>e</sup> Institute of Marine Science, Federal University of São Paulo, Santos, Brazil

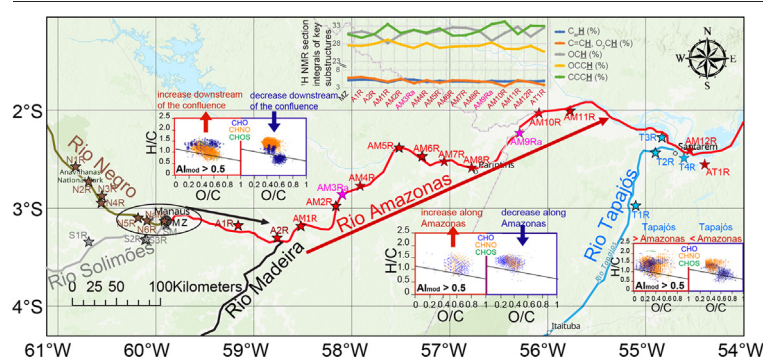
<sup>f</sup> Program in Geosciences – Environmental Geochemistry, Chemistry Institute, Fluminense Federal University, 24020-141 Niteroi, Brazil

<sup>g</sup> Department of Environmental Sciences, University of Toledo, Toledo, OH 43606, USA

## HIGHLIGHTS

- Unveiling DOM molecular and structural characteristics in the Amazon basin
- ESI[±] FT-ICR MS and NMR provided comprehensive coverage of DOM processing.
- Nitrogen containing molecules are critical partners in the cycling of DOM.
- DOM in the Amazon River mixing zones showed non-conservative behavior.
- Physicochemical and microbial processes determine DOM changes in the Amazon basin.

## GRAPHICAL ABSTRACT



## ARTICLE INFO

Editor: Shuzhen Zhang

### Keywords:

Mixing zone  
Tributaries  
Environmental drivers  
FT-ICR MS  
NMR

## ABSTRACT

Rivers are natural biogeochemical systems shaping the fates of dissolved organic matter (DOM) from leaving soils to reaching the oceans. This study focuses on Amazon basin DOM processing employing negative and positive electro-spray ionization Fourier transform ion cyclotron resonance mass spectrometry (ESI[±] FT-ICR MS) and nuclear magnetic resonance spectroscopy (NMR) to reveal effects of major processes on the compositional space and structural characteristics of black, white and clear water systems. These include non-conservative mixing at the confluences of (1) Solimões and the Negro River, (2) the Amazon River and the Madeira River, and (3) in-stream processing of Amazon River DOM between the Madeira River and the Tapajós River. The Negro River (black water) supplies more highly oxygenated and high molecular weight compounds, whereas the Solimões and Madeira Rivers (white water) contribute more CHNO and CHOS molecules to the Amazon River main stem. Aliphatic CHO and abundant CHNO compounds prevail in Tapajós River DOM (clear water), likely originating from primary production. Sorption onto particles and heterotrophic microbial degradation are probably the principal mechanisms for the observed changes in DOM composition in the Amazon River and its tributaries.

*Abbreviations:* S-DOM, PPL-based solid phase extracted dissolved organic matter (SPE-DOM) from the Solimões River; A-DOM, SPE-DOM from the Amazon River; N-DOM, SPE-DOM from the Negro River; T-DOM, SPE-DOM from the Tapajós River.

\* Corresponding author.

E-mail address: [hertkorn@helmholtz-muenchen.de](mailto:hertkorn@helmholtz-muenchen.de) (N. Hertkorn).

<http://dx.doi.org/10.1016/j.scitotenv.2022.159620>

Received 19 July 2022; Received in revised form 15 September 2022; Accepted 17 October 2022

Available online 21 October 2022

0048-9697/© 2022 Published by Elsevier B.V.

## 1. Introduction

The Amazon River catchment is the largest river system in the world, responsible for ~20 % of the global freshwater discharge and exports of ~35 Tg organic carbon (of which 60–70 % is dissolved) annually to the world's oceans (Moreira-Turcq et al., 2003a). The river system is the ultimate driver of aquatic life in the region and a key connector between terrestrial organic carbon and its mineralization (Battin et al., 2009; Cole et al., 2007). Riverine dissolved organic matter in the Amazon River and its tributaries (AZ-DOM) is involved in critical ecosystem processes, such as nutrient availability, growth efficiency of aquatic organisms, decomposition rate of plant debris, and ultimately, the carbon cycle (Drake et al., 2021; Santos-Junior et al., 2020). Therefore, ecosystem-wide understanding of dissolved organic matter (DOM) molecular composition and structures is needed to comprehend key biogeochemical processes in the Amazon basin.

Previous studies on the origin and fate of organic matter (OM) in the Amazon River included stable isotope (Mortillaro et al., 2011; Quay et al., 1992) and radioisotope analysis (Hedges et al., 1986) to assess sources and age of organic carbon. Quantification of targeted compounds involved humic substances (Ertel et al., 1986), saccharides (Salot et al., 2001) and amino acids (Hedges et al., 1994), among others. Optical spectroscopy (Martinez et al., 2015), mass spectrometry (Gonsior et al., 2016) and  $^{13}\text{C}$  NMR spectroscopy (Hedges et al., 1992) were applied to understand the composition of its OM. Incubation experiments measured the rates of primary production (Gagne-Maynard et al., 2017), biological (Benner et al., 1995) and photo-degradation (Amado et al., 2006; Amon and Benner, 1996) in the Amazon River. However, comprehensive molecular understanding of AZ-DOM reactivity and bioavailability, and assessment of its biotic and abiotic processing is lacking at present, especially in tributaries with different water types and in major confluence zones.

Many ungauged tributaries with specific biogeochemical characteristics enter the Amazon River which have long been classified into three types according to their appearance: “Blackwaters” that are relatively acidic (pH ~ 5), low in total cations and rich in DOM, such as the Negro River, “Whitewaters” that show a near-neutral pH and are relatively rich in total cations and in suspended sediments, such as Solimões and Madeira River, and “Clearwaters” which exhibit low suspended sediment loads, and high light transparency, such as Tapajós River (McClain and Naiman, 2008). Different water types in the Amazon basin have been shown to have distinct DOM compositions (Gonsior et al., 2016). Solimões and Negro combine in Manaus to form the Amazon River (turbid water). Madeira (DOC ~5.8 mg/L, POC ~ 0.83 mg/L) joins the Amazon River downstream at ~140 km east of Manaus (do Nascimento et al., 2015). Tapajós River drains into the Amazon River at the town of Santarem (~620 km from Manaus). Mixing of different water types initiates complex biogeochemical processing, including alteration of aquatic microbial communities and food webs (Lynch et al., 2019), DOM itself (Bianchi and Ward, 2019), and of river bulk characteristics.

Amazon River is a net heterotrophic ecosystem in which respiration far exceeds primary production (Hedges et al., 1994), and most  $\text{CO}_2$  outgassing originates from allochthonous carbon (Abril et al., 2014; Mayorga et al., 2005; Richey et al., 2002). Clear rivers show comparatively higher primary production, as solar radiation exposure decreases due to high aromatic DOM content in black rivers and turbidity from high sediment loads in white rivers (Moreira-Turcq et al., 2003a). Bacterial and photochemical processing and mineralization as well as chemoselective sorption to minerals are the defining processes determining OM biogeochemistry in the Amazon catchments (Amon and Benner, 1996; Armanious et al., 2014; Moreira-Turcq et al., 2003b; Pérez et al., 2011; Shen, 1999).

Polydispersity, heterogeneity, and temporal dynamics of DOM have made its molecular characterization a long-standing challenge. This study employs complementary negative and positive electrospray ionization ESI [ $\pm$ ] FT-ICR MS to determine chemical composition out of the AZ-DOM with excellent coverage of CHO, CHNO, and CHOS molecules (Hertkorn et al., 2016, 2013). 800 MHz  $^1\text{H}$  NMR spectroscopy provided quantification

of major atomic environments in DOM molecules with excellent S/N ratio and resolution, enabling quantification of key DOM structural units including aliphatic and carboxyl-rich alicyclic molecules (CRAM), oxygenated aliphatics including carbohydrates, olefins, and aromatics (Hertkorn et al., 2013, 2016; Powers et al., 2019; Simpson et al., 2011). Bulk characterization of Amazon waters in conjunction with selected incubation experiments further contributed to dissecting relevant aspects of DOM processing.

## 2. Material and methods

### 2.1. Sampling and site locations

We collected water samples at 31 sites in the Amazon River main stem eastwards, including Solimões (white water), Negro (black water), Amazon (turbid water), and Tapajós (clear water) (Figs. 1, S1 and Table S1) between April 2<sup>nd</sup> and May 25<sup>th</sup> in 2014, during a high-water period with very high discharge volume. Sampling coordinates and information, as well as isolated DOM by PPL-based solid phase extraction (SPE-DOM; Dittmar et al., 2008) of the water samples are described in the Supplementary information (SI).

### 2.2. FT-ICR mass spectrometry

Negative and positive electrospray ionization (ESI [ $\pm$ ]) Fourier transform ion cyclotron resonance mass spectra (FT-ICR MS) were acquired using a 12 T Bruker Solarix mass spectrometer (Bruker Daltonics, Bremen, Germany) and an Apollo II electrospray ionization (ESI) source (Hertkorn et al., 2016). Data processing used Compass Data Analysis 4.1 (Bruker, Bremen, Germany) and formula assignment used an in-house made software (NetCalc) (Tziotis et al., 2011); further details are described in SI. Intensity-weighted average bulk parameters such as  $m/z$  and atomic ratios (e.g., O/C, H/C, S/C, N/C) were computed from ESI [ $\pm$ ] FT-ICR MS of AZ-DOM (Tables 1, S3, S4). A modified aromaticity index ( $\text{AI}_{\text{mod}}$ ) was computed by considering only half of the oxygen being present in carbonyl functional groups by the equation:  $\text{AI}_{\text{mod}} = (1 + \text{C} - 0.5\text{O} - \text{S} - 0.5\text{H}) / (\text{C} - 0.5\text{O} - \text{S} - \text{N} - \text{P})$  (Koch and Dittmar, 2006). The total intensity of  $m/z$  ions in each sample that had  $\text{AI}_{\text{mod}} > 0.5$ , an indicator of aromatic structures, was computed and shown in Tables. 1, S3, S4.

### 2.3. $^1\text{H}$ NMR spectroscopy

800 MHz  $^1\text{H}$  NMR spectra of AZ-DOM were acquired with a Bruker Avance III NMR spectrometer operating at 800.35 MHz ( $B_0 = 18.8$  Tesla) at 283 K from redissolved solids in  $\text{CD}_3\text{OD}$  as described in SI.

### 2.4. Water characterization

Water conductivity (Cond.), temperature (Temp.) and dissolved oxygen (DO) were measured in situ with a portable instrument (Hanna Instruments, Metrohm electrode and PRO-ODO YSI). Inorganic nutrients, DOC, particulate organic carbon (POC), dissolved inorganic carbon (DIC), and pH were determined by standard procedures as described in SI.

### 2.5. Dark carbon fixation (DCF) and heterotrophic bacterial production (HBP)

DCF and HBP are important microbial processes that supply fresh bio-material to both DOC and POC. DCF was determined by the incorporation of  $^{14}\text{CO}_2$  in a known time, and HBP was determined by the measurement of protein incorporation of radio-labelled  $^3\text{H}$ -Leucine as described in SI.

### 2.6. Statistical analysis

Data mining and the application of multivariate statistics served to analyze these complex sets of complementary data. Principal component analysis (PCA) was performed using Simca-P (version 11.5, UmetricsAB, Umeå, Sweden). Hierarchical Cluster Analysis (HCA) was performed using Hierarchical Clustering Explorer 3.0. Spearman correlation analysis ( $p < 0.05$ ,  $r^2 > 0.5$ )

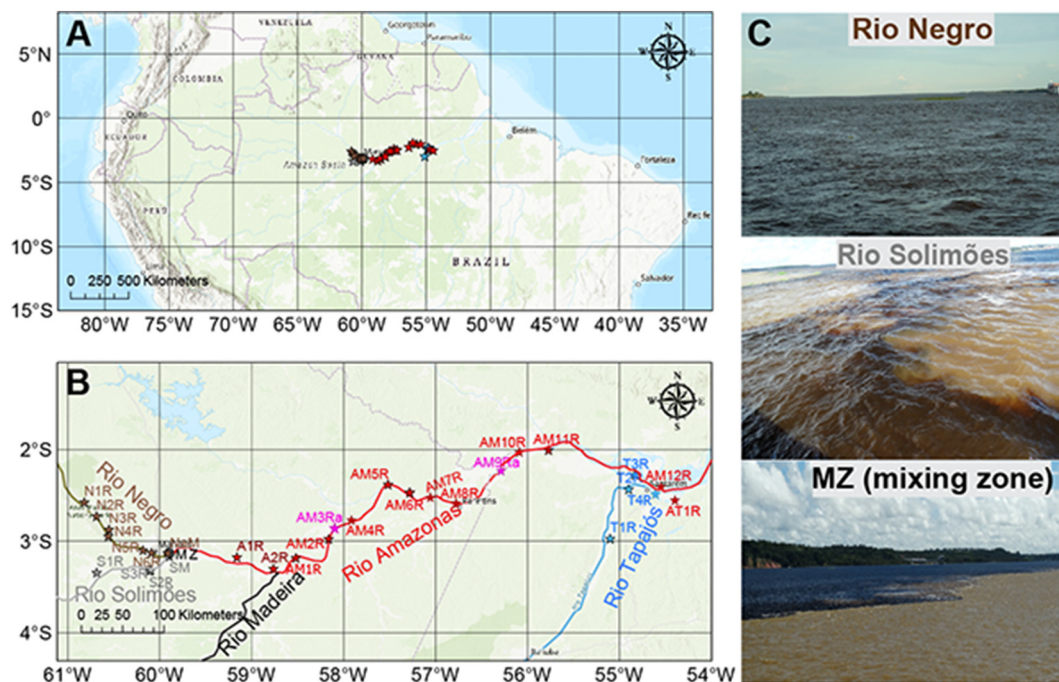


**Fig. 1.** Maps A, B and own photographs C of the sampling sites in the Amazon River. MZ (black) was sampled at the mixing zone of the Solimões River (grey) and the Negro River (brown). A1R/A2R (dark red) were sampled in the Amazon River upstream of the Madeira River inflow, while the other Amazon River samples (red) were sampled downstream of the Madeira River inflow. AM3Ra and AM9Ra (magenta) were sampled two months later than the other water samples. The enlarged view of panel B is shown in Fig. S1.

was performed using the R statistical platform. Non-metric multidimensional scaling (NMDS) analysis was performed using the R statistical platform with the package *vegan* to determine correlations of environmental variables with DOM molecular composition in the Amazon River continuum. Expanded descriptions of the statistical analyses are included in SI.

### 3. Results

#### 3.1. High diversity of AZ-DOM revealed by ESI[±] FT-ICR MS and <sup>1</sup>H NMR

ESI[±] FT-ICR MS of all AZ-DOM samples showed distinct distributions of thousands of negative/positive molecular signatures covering the *m/z* range 150–950, indicating considerable ionization selectivity but high complementarity (Figs. 2, S2) (Hertkorn et al., 2008, 2013). Overall, ESI[−] FT-ICR MS preferentially detected high-mass oxygen-rich CHO compounds, whereas ESI[+] FT-ICR MS primarily detected aliphatic CHNO compounds. Nearly half of CHO and CHNO molecular compositions were

found in both ESI[±] modes at near-average H/C and O/C atomic ratios for which the count of feasible isomeric molecules is maximal (Hertkorn et al., 2007). Moreover, CHOS compounds were better ionized in ESI[−] than in ESI[+], and CHNOS compounds were almost absent. All <sup>1</sup>H NMR spectra of AZ-DOM showed smooth bulk envelopes (Fig. S3), reflecting superpositions of millions of atomic environments typical of processed aqueous DOM (Hertkorn et al., 2013).

#### 3.2. Decreased abundance of oxygen-rich aromatic DOM molecules downstream of the Solimões-Negro mixing zone

DOC and nitrate (NO<sub>3</sub><sup>−</sup>) concentrations were higher in Negro, whereas POC, DIC, and nitrite (NO<sub>2</sub><sup>−</sup>) concentrations, as well as discharge, conductivity, and pH were higher in Solimões (Table S2). DOC and DIC concentrations in Amazon River ranged between those in Solimões and Negro, consistent with previous studies, whereas ~90% of POC was lost at the Solimões-Negro (SN)-confluence, much larger than described in previous

**Table 1**

ESI[±] FT-ICR MS derived counts of mass peaks and intensity-weighted average bulk parameters for all assigned masses occurring in AZ-DOM. This table shows value ranges for DOM in Negro, Solimões, Amazon, and Tapajós main stem, respectively; values for each sample see Tables S3–S4.

FT-ICR MS	Sample	Total counts of mass peaks	CHO %	CHNO %	CHOS %	CHNOS %	<i>m/z</i>	DBE/C	H/C	O/C	N/C × 10 <sup>−2</sup>	S/C × 10 <sup>−5</sup>	Al <sub>mod</sub> > 0.5 %
ESI[−]	Negro	3781–4519	73.2–76.9	21.8–25.2	1.35–1.73	0.00–0.03	477.1–498.3	0.52–0.53	1.04–1.06	0.53–0.55	0.3–0.4	20.7–40.4	14.3–16.7
	Solimões	4759–5043	59.5–63.6	31.0–32.4	5.33–7.20	0.00–0.04	460.2–482.5	0.52–0.53	1.06–1.07	0.54–0.55	0.6–0.8	93.7–112.3	13.7–15.7
	Amazon	4120–5010	63.0–70.3	26.7–30.7	3.05–6.31	0.00–0.34	467.9–488.9	0.51–0.52	1.05–1.07	0.53–0.55	0.5–0.7	43.4–100.5	13.2–15.4
	Tapajós	5276–5898	57.9–62.4	32.1–35.3	3.87–6.93	0.04–2.24	446.6–472.1	0.49–0.52	1.08–1.11	0.51–0.53	0.7–0.8	82.7–120.7	12.0–14.6
	NaM	3781	76.9	21.8	1.35	0.00	498.3	0.53	1.04	0.54	0.3	17.2	16.6
	SM	4408	65.7	29.0	5.08	0.16	479.9	0.52	1.06	0.54	0.6	78.7	14.9
	MZ	4424	73.4	24.8	1.79	0.00	492.4	0.52	1.05	0.53	0.3	22.8	15.5
ESI[+]	Negro	4824–5973	28.4–30.9	68.9–71.4	0.05–0.15	0.00–0.04	438.4–454.8	0.39–0.40	1.32–1.36	0.40–0.43	3.5–3.8	2.5–5.3	2.0–2.8
	Solimões	3817–4967	29.5–31.3	68.5–70.2	0.08–0.18	0.00–0.18	425.2–439.2	0.38–0.40	1.34–1.37	0.36–0.41	3.7–3.9	2.3–5.0	2.5–3.3
	Amazon	3477–6160	27.7–34.6	65.1–71.6	0.03–0.61	0.00–1.45	380.89–422.8	0.39–0.41	1.32–1.38	0.36–0.42	3.5–4.3	2.3–16.9	2.4–5.0
	Tapajós	3564–4709	29.6–32.3	67.5–70.3	0.07–0.19	0.02–0.24	386.67–397.6	0.39–0.40	1.35–1.37	0.38–0.39	3.9–4.1	2.8–5.6	3.5–4.5
	NaM	5428	28.9	70.9	0.15	0.02	439.2	0.39	1.36	0.39	3.7	3.4	2.6
	SM	5172	28.5	71.0	0.19	0.27	413.2	0.38	1.38	0.37	4.0	6.2	3.1
	MZ	5808	28.6	71.2	0.17	0.03	437.7	0.38	1.38	0.39	3.8	5.0	2.1

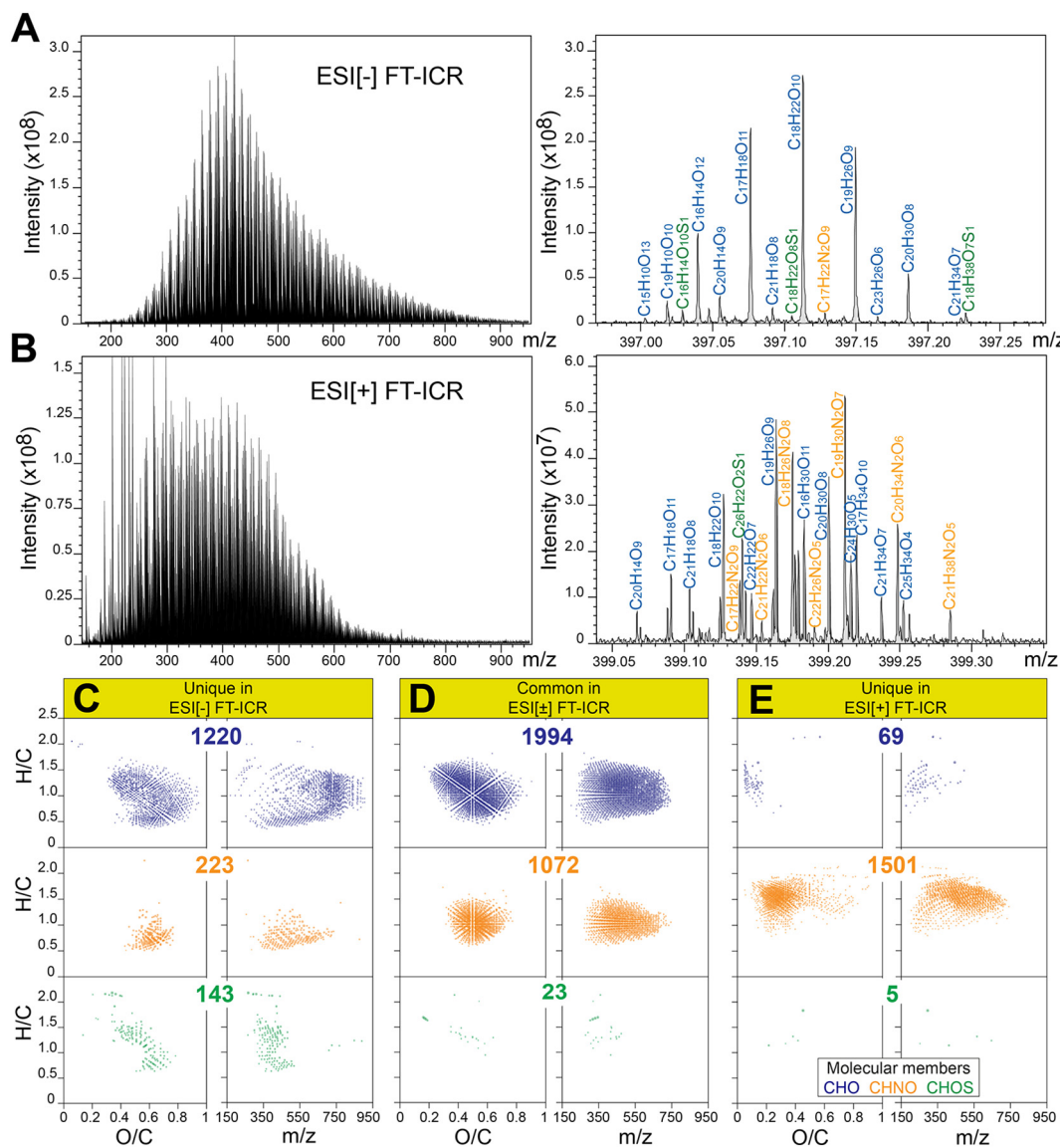


**Fig. 2.** ESI[ $\pm$ ] FT-ICR mass spectra and comparison of their identified molecular compositions exemplified with the Amazon River sample A1R. The A ESI[ $-$ ] and B ESI[ $+$ ] FT-ICR MS spectra showed distinct distributions of mass peaks across a wide mass range ( $m/z$  150–950), as well as signatures at nominal mass 398 confirming relevant ionization selectivity. Respective assignments of molecular compositions are provided for CHO (blue), CHNO (orange), and CHOS (green) molecules. Van Krevelen and mass-edited  $m/z$  diagrams of C the molecular formulae identified only in ESI[ $-$ ] FT-ICR MS; D the molecular formulae identified in both ESI[ $\pm$ ] FT-ICR MS; E the molecular formulae identified only in ESI[ $+$ ] FT-ICR MS. Numbers show counts of assigned formulae.

studies (Moreira-Turcq et al., 2003b). Furthermore, dissolved oxygen (DO) at Solimões-Negro confluence and the Amazon upstream was  $\sim 30\%$  lower than in Solimões and Negro (Table S2), a larger change than previously shown (Quay et al., 1995).

Comparison of MS-derived average parameters revealed cumulative alterations of molecular compositions (Tables 1, S3, S4). The ESI[ $\pm$ ] FT-ICR MS-derived average N/C and S/C atomic ratios were higher in S-DOM than in N-DOM. All MS-derived bulk parameters of DOM close to Solimões-Negro mixing zone (MZ) and A-DOM ranged between those of the N-DOM and S-DOM just upstream of the very mixing zone (NaM and SM). The more downstream A-DOM showed declined average CHO%, O/C and  $m/z$  ratios compared to MZ.

$^1\text{H}$  NMR derived section integrals showed higher content of aromatic ( $\text{C}_{\text{ar}}\text{H}$ ;  $\delta_{\text{H}} \sim 7.0\text{--}10.0$  ppm) and olefinic units ( $=\text{CH}$ ;  $\delta_{\text{H}} \sim 5.3\text{--}7.0$  ppm) in N-DOM, while pure aliphatic protons ( $\text{CCCH}$  units,  $\delta_{\text{H}} \sim 0.5\text{--}1.25$  ppm) were more abundant in S-DOM (Tables 2, S5); direct oxygenated units ( $\text{OCH}$ ;  $\delta_{\text{H}} \sim 3.5\text{--}4.9$  ppm) and remotely oxygenated aliphatic units ( $\text{OCCCH}$ ;  $\delta_{\text{H}} \sim 1.9\text{--}3.2$  ppm) showed near equal relative abundance in the

N-DOM and S-DOM just upstream of Solimões-Negro mixing zone.  $^1\text{H}$  NMR section integrals of key substructures in MZ, A1R, and A2R were more similar to N-DOM, while that of more downstream A-DOM were closer to S-DOM.  $^1\text{H}$  NMR section integrals of aromatic, olefinic, and oxygenated protons showed declining trend from A1R to AM1R, in line with our FT-ICR MS results showing declining average O/C, DBE/C, and  $m/z$  ratios, whereas H/C ratios and relative abundance of the total aliphatics ( $\text{OCCCH}$ ,  $(\text{CH}_2)_n$ ,  $\text{CCCH}_3$ ;  $\delta_{\text{H}} \sim 0.5\text{--}1.9$  ppm) increased in this reach (Tables S3–S5), suggesting increase of aliphaticity.

We performed unsupervised multivariate statistics on ESI[ $\pm$ ] FT-ICR MS and  $^1\text{H}$  NMR derived compositional and structural features to analyze the alteration of the DOM composition upstream and downstream of Solimões-Negro confluence. In both ESI[ $\pm$ ] FT-ICR MS-based PCA, the first principal components (PC1) showed clear separation as follows: N-DOM  $\sim$  MZ < A1R/A2R < S-DOM  $\sim$  more downstream A-DOM < AM1R (Fig. 3A, B). Van Krevelen and mass-edited H/C diagrams illustrate PCA loadings and show key molecular features differentiating AZ-DOM. The molecular composition with positive/negative loading vector corresponds to higher/lower

**Table 2**

$^1\text{H}$  NMR section integrals (percent of non-exchangeable protons) and key substructures of AZ-DOM ( $\text{CD}_3\text{OD}$ , exclusion of residual water, and methanol). This table shows value ranges for DOM in Negro, Solimões, Amazon, and Tapajós main stem, respectively; values for each sample see Table S5. The fundamental substructures include aromatics  $\text{C}_{ar}\text{H}$ ,  $\delta_{\text{H}} \sim 7.0\text{--}10.0$  ppm; olefins =  $\text{CH}_2$  and  $\text{O}_2\text{CH}$  units,  $\delta_{\text{H}} \sim 5.3\text{--}7.0$  ppm; oxygenated aliphatics  $\text{OCH}$  units,  $\delta_{\text{H}} \sim 3.2\text{--}4.9$  ppm; “acetate-analogue” and CRAM,  $\delta_{\text{H}} \sim 1.9\text{--}3.2$  ppm; functionalized aliphatics,  $\delta_{\text{H}} \sim 1.35\text{--}1.9$  ppm; polyethylene group,  $\delta_{\text{H}} \sim 1.25\text{--}1.35$  ppm; pure aliphatics,  $\delta_{\text{H}} \sim 0.5\text{--}1.25$  ppm.

$\delta$ ( $^1\text{H}$ ) [ppm]	10.0–7.0	7.0–5.3	4.9–3.2	3.2–1.9	1.9–1.35	1.35–1.25	1.25–0.5	1.9–0.5
Key substructures	$\text{C}_{ar}\text{H}$ (%)	$\text{HC}=\text{C}$ , $\text{HCO}_2$ (%)	$\text{HCO}$ (%)	$\text{HCCO}$ (%)	$\text{HC-C-O}$ (%)	$(\text{CH}_2)_n$ (%)	$\text{HCCC}$ (%)	Total aliphatic section (%)
Negro	5.0–5.7	5.7–6.9	29.9–33.8	27.1–28.0	13.1–14.6	3.6–4.2	9.8–12.2	27.0–30.4
Solimões	4.6–5.6	4.3–5.6	31.1–33.1	25.7–27.1	14.1–14.8	3.9–4.7	12.2–14.0	30.4–33.3
Amazon	4.5–5.3	3.4–6.0	28.2–32.8	26.5–29.1	14.1–15.9	4.0–4.8	11.5–14.7	29.7–34.2
Tapajós	4.8–4.9	4.0–6.7	27.3–32.8	26.0–28.1	14.2–15.2	4.7–5.4	11.9–15.5	30.8–35.1
NaM	5.5	5.7	30.2	27.6	14.6	4.2	12.2	31.0
SM	4.9	4.0	29.5	27.2	15.1	5.0	14.3	34.4
MZ	5.1	5.8	30.9	27.5	14.7	4.4	11.5	30.6

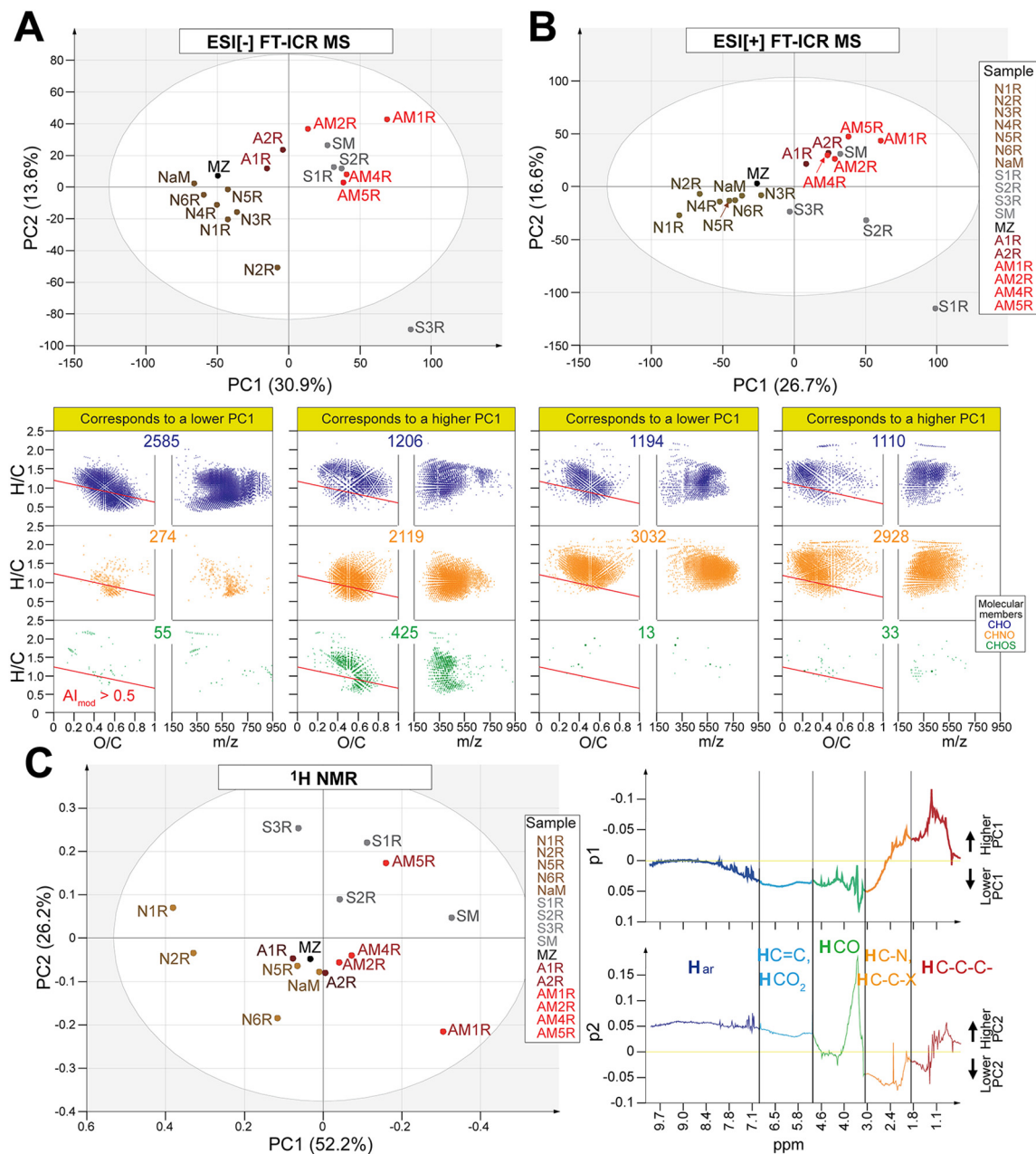


**Fig. 3.** PCA of AZ-DOM upstream/downstream of the Solimões-Negro mixing zone based on all assigned molecular formulae in ESI[ $\pm$ ] FT-ICR MS and  $^1\text{H}$  NMR spectra. The upper panels show PCA scatter plots based on A ESI[ $-$ ] and B ESI[ $+$ ] FT-ICR MS, respectively. The lower panels of A and B show the van Krevelen and mass-edited H/C diagrams corresponding to lower/higher PC1, with the color code representing elemental composition (i.e., CHO (blue), CHNO (orange), and CHOS (green)). Molecular compositions positioned below the red lines in the van Krevelen diagrams have  $\text{AI}_{\text{mod}} < 0.5$  (Koch and Dittmar, 2006). Numbers show counts of assigned formulae. The right panel of C shows loading vectors p1/p2 of PC1/PC2, with fundamental substructures within the  $^1\text{H}$  NMR spectra indicated.

principal components, respectively. ESI[±] FT-ICR MS-based PCA showed large-scale loss of high molecular weight, more oxygenated and more unsaturated CHO and CHNO DOM molecules at Solimões-Negro confluence. A large proportion of attenuated CHO compounds had  $AI_{mod} > 0.5$  (Koch and Dittmar, 2006), which is an indicator of aromatic structures. The declined CHNO compounds had lower average  $AI_{mod}$  than the CHO compounds, but were highly oxygenated and ionized in both ESI[±] modes. Highly oxygenated CHOS compounds were more abundant in S-DOM/A-DOM than in N-DOM and covered large areas in van Krevelen diagrams, indicative of considerable molecular diversity. For the interpretation of other principal components see Fig. S4. Moreover, HCA separated AZ-DOM alike PCA (Fig. S5). A1R and MZ clustered together with N-DOM in ESI[−] due to higher abundance of polyphenolic CHO-compounds, whereas MZ clustered together with N-DOM in ESI[+] because of more oxygen-rich CHNO compounds ( $m/z$  500–750). A-DOM and S-DOM clustered together with higher content of oxygenated CHO/CHOS compounds and less oxygenated CHNO compounds ( $m/z$  300–550).

$^1H$  NMR based-PCA showed the structural differences of AZ-DOM proximate to Solimões-Negro mixing zone that were elucidated by NMR loading plots (Fig. 3C). N-DOM showed lower PC1 because of more protons bound to  $sp^2$ -hybridized carbon, as well as OCH units, at the expense of lower relative abundance in pure and remotely oxygenated substituted aliphatic units. Moreover, S-DOM, N1R, and AM5R (sampled just downstream of the Uatumã River inflow; black water) showed higher second principal components (PC2) due to higher content of polycarboxylated aromatic compounds or certain heterocyclic structures, as well as OCH units. AM5R was separated in  $^1H$  NMR based-PCA (Fig. 3C) but not in FT-ICR MS-based PCA (Fig. 3A, B), possibly because the abundant aromatic or heterocyclic structures in AM5R contained few ionizable substituents.

### 3.3. Madeira inflow supplies oxygen-poor CHO molecules and heteroatom-containing compounds to the Amazon River

The Madeira River is an important tributary that supplies a large amount of sediment to the Amazon River. A-DOM just downstream of Madeira (AM1R) showed the highest content of CHNO/CHOS compounds and the lowest average  $m/z$  in A-DOM (Tables S3–S4), and was separated in ESI[±] FT-ICR MS-based PCA (Fig. 3A, B). Furthermore, AM1R was separated in ESI[−] FT-ICR MS-based HCA (Fig. S6-a4) due to higher abundance in oxygenated CHO/CHNO/CHOS compounds ( $m/z$  250–550), and in ESI[+] FT-ICR MS-based HCA (Fig. S6-b3) due to higher abundance in less oxygenated and more saturated CHO/CHNO compounds ( $m/z$  250–550). Moreover, AM4R (sampled out of the river main stem where water overflowed the bank) showed distinction due to high content of unsaturated CHO/CHNO compounds, which likely originated from adjacent floodplains. In addition, A1R and A2R clustered together due to higher abundance of polyphenolic and some oxygenated aliphatic CHO compounds ( $m/z$  400–900) (Fig. S6-a1), and some oxygenated CHNO compounds ( $m/z$  400–750) (Fig. S6-b1).

AM1R showed higher  $^1H$  NMR section integrals of pure and functionalized aliphatic compounds but lower integrals of aromatic, olefinic, and OCH units, compared to other A-DOM (Table S5, Fig. S7). These molecular features caused the distinction of AM1R in NMR-derived PCA (Fig. 3C), opposite to N-DOM. Moreover, AM4R showed higher abundance of OCH units than the other upstream A-DOM (Table S5, Fig. S7).

### 3.4. Changes of DOM composition along the Amazon River

The  $m/z$  ions of each A-DOM in ESI[−] or ESI[+] FT-ICR MS showed similar patterns in van Krevelen and mass-edited H/C diagrams alike A1R (Fig. 2), ~70 % of which were common in all A-DOM (Fig. S8-a3, b3). ESI[±] FT-ICR MS-derived bulk parameters and PCA indicated non-linear trends of DOM composition along the Amazon River (Tables S3–S4, Fig. 4A, B). AM1R was outside the 95 % confidence interval of ESI[−] MS-based PCA (Fig. 4A). AM2R was more similar to A-DOM just downstream of Solimões-Negro confluence (Fig. 4A, B). Moreover, AM12R,

AM3Ra, and AM9Ra showed higher PC1 with higher abundance in polyphenolic and highly oxygenated CHO compounds (Fig. 4A), as well as higher abundance of less oxygenated CHO/CHNO compounds (Fig. 4B). For the interpretation of PC2 see Fig. S9.

$^1H$  NMR section integrals of A-DOM showed non-continuous trends as well, except that the relative abundance of purely aliphatic CCH units increased from A1R to AM1R and from AM6R to AM10R (Table S5). A1R and A2R showed higher PC1 in  $^1H$  NMR-based PCA (Fig. 4C), which refers to more abundant functionalized units including alkylated and oxygen-rich aromatic molecules, conjugated double bonds, and various oxygen-rich aliphatics. A-DOM from AM6R to AM10R showed declining PC1 in  $^1H$  NMR-based PCA (Fig. 4C) that were not observed in ESI[±] FT-ICR MS-based PCA (Fig. 4A, B). Furthermore, PC2 separated AM1R from due to higher content of remotely oxygenated and branched aliphatic protons.

Spearman correlation analysis was performed on MS-derived molecular compositions of A-DOM from AM1R to AM10R (Fig. S9). Molecular signatures showing positive/negative correlation with distance from AM1R had similar  $m/z$  but distinct O/C ratios. In both ESI[−] and ESI[+] MS-based analyses, less oxygenated CHO/CHO compounds became depleted downstream (Fig. S10-a2, b2) whereas more oxygenated CHO/CHNO compounds accumulated downstream (Fig. S10-a2, b2).

### 3.5. The comparison of S/N/A/T-DOM

The common mass peaks in S/N/A/T-DOM showed similar patterns (Fig. S8), with CHO<sub>14–15</sub>, CHNO<sub>8–9</sub>, and CHO<sub>8–10</sub>S compounds being most abundant (Fig. S11), indicating that AZ-DOM molecules were overall higher oxygenated compared to other riverine DOM (Bae et al., 2011). S-DOM contained ~600 oxygenated CHNO/CHOS compounds not observed in N-DOM (Fig. S12A), while N-DOM contained CHO and CHNO compounds with  $m/z > 450$  not observed in S-DOM (Fig. S12B). Moreover, 124  $m/z$  ions unique to MZ were not found in S-DOM/N-DOM, most of which were CHNO compounds of higher aliphaticity (Fig. S12C). The counts of molecular formulae in each T-DOM in ESI[−] MS were approximately 38 %/27 %/18 % higher than in S/N/A-DOM, respectively. Molecular formulae unique to T-DOM represented less oxygenated CHO/CHNO compounds in a wide  $m/z$  range 300–800 (Fig. S13A), and were positioned in van Krevelen space like abundant mass peaks in exudates from phytoplankton (Medeiros et al., 2015). Meanwhile, counts of molecular formulae in T-DOM from ESI[+] MS were ~20 % lower than in S/N/A-DOM. The ions absent in T-DOM were attributed to CHNO compounds with  $m/z > 600$  (Fig. S13B). Overall, S-DOM had highest content of S-containing compounds and T-DOM had highest content of N-containing compounds (Tables 1, S3, S4). Additionally, T-DOM had lowest average  $m/z$  and O/C, and highest average H/C ratios, consistent with previous studies (Seidel et al., 2016), and indicative of earlier stages of DOM processing.

$^1H$  NMR spectra of N-DOM were distinct and showed higher levels of oxygenation in all aliphatic and aromatic substructures (Fig. S3).  $^1H$  NMR spectra of S-DOM and T-DOM showed lower proportions of aromatic units and higher content of aliphatic units than A-DOM and N-DOM (Fig. S3).

T-DOM was distinct in ESI[−] FT-ICR MS-based PCA by PC1 due to higher content of more saturated, less oxygenated CHO/CHOS compounds and highly unsaturated CHNO/CHOS compounds (Fig. S14A). However, the distinction of T-DOM did not appear in ESI[+] FT-ICR MS-based PCA (Fig. S14B). Additionally, upstream T-DOM and upstream S-DOM were separated out by PC2 in ESI[−] and ESI[+] FT-ICR MS-based PCA, respectively, due to higher content of less oxygenated compounds (Fig. S15).

$^1H$  NMR-based PCA (Fig. S16A) showed similar separation in PC1 direction alike ESI[±] FT-ICR MS-based PCA. The  $^1H$  NMR loading spectra showed that the main differences between S/N/A/T-DOM resided in the overall unsaturation and oxygenation, covering the entire aromatic and aliphatic units (Fig. S16B). T4R (very close to Amazon) was outside the 95 % confidence interval because of its huge  $^1H$  NMR resonances representing purely aliphatic protons.

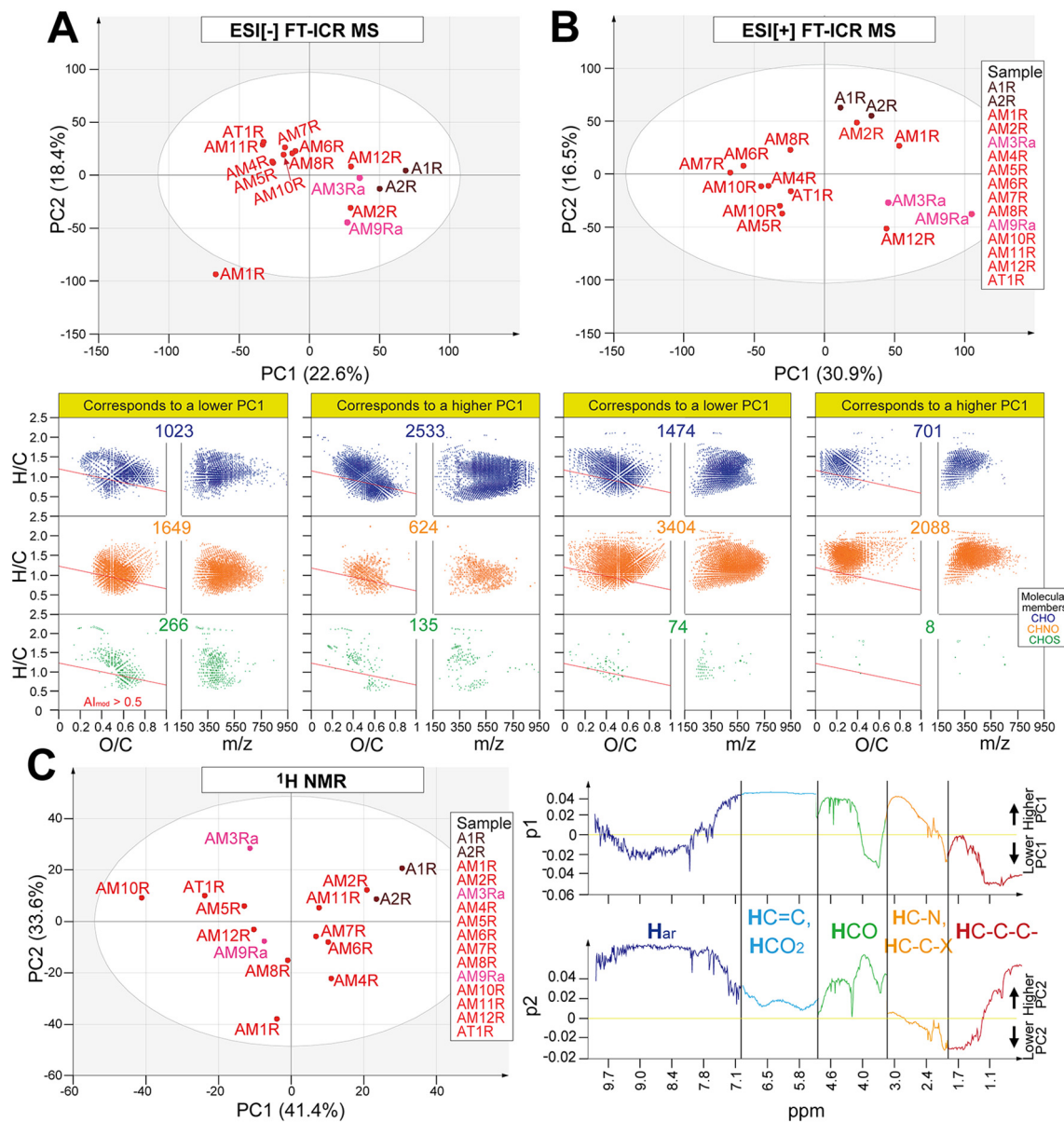


**Fig. 4.** PCA of A-DOM based on all assigned molecular formulae in ESI [±] FT-ICR MS and  $^1\text{H}$  NMR spectra. The upper panels show the distribution of A-DOM in PCA scatter plots based on A ESI [−] and B ESI [ + ] FT-ICR MS, respectively. The lower panels of A and B shows the van Krevelen and mass-edited H/C diagrams corresponding to lower/higher PC1, with the color code representing elemental composition (i.e., CHO (blue), CHNO (orange), and CHOS (green)). Molecular compositions positioned below the red lines in the van Krevelen diagrams have  $A_{I_{mod}} < 0.5$  (Koch and Dittmar, 2006). Numbers show counts of assigned formulae. The right panel of C shows loading vectors  $p_1/p_2$  of PC1/PC2, with fundamental substructures within the NMR spectra indicated.

### 3.6. Factors regulating AZ-DOM composition

Microbial metabolic processes are suitable biological parameters to understand microbial roles on organic matter decomposition and ecosystem functions (Kamjunke et al., 2015). For instance, HBP refers to assimilatory metabolism consuming preferentially labile DOM like proteins (Seidel et al., 2015). DCF is inorganic light independent C-uptake, mostly performed by chemosynthetic microorganisms, using redox reactions energetic yields to recycle inorganic carbon (Santoro et al., 2013). DCF in A1R was ~15 times higher than in sites upstream of this very mixing zone and A2R (Table S6). Moreover, HBP in A2R was ~6 times of A1R and was >20 times compared to in Negro and Solimões (Table S6). The rate of DCF was ~4 times higher than HBP in A1R, whereas was only 4 % of HBP in A2R. These results suggested that the incorporation of inorganic carbon and labile organic carbon could be highly variable and DCF may play an unexpectedly important role for microorganisms at Solimões-Negro mixing zone.

We performed ESI [±] FT-ICR MS and  $^1\text{H}$  NMR-based NMDS analysis to elucidate the factors influencing the molecular composition of AZ-DOM (Fig. S17; Table, S7). DOC, POC, DIC, and conductivity differentiated S-DOM and N-DOM, showing that the distinct water characteristics of the two end-member rivers likely result in its SPE-DOM composition. In addition, DOC concentration and pH were the major factors differentiating upstream A-DOM (A1R and A2R) from downstream A-DOM in ESI [−] MS-based NMDS, whereas the other parameters did not show significant correlations (Fig. S17, Table S7). However, pH did not separate downstream A-DOM, suggesting that pH did not have strong effects on DOM composition downstream of the Amazon River (Fig. S17). Inorganic nutrient concentrations did not show significant correlations with AZ-DOM composition (Table S7), likely because of their very low abundances (mostly <1  $\mu\text{M}$ ; Table S2). Furthermore, we performed the same NMDS method on the samples for which HBP and DCF were measured (Fig. 5, Table S8) and HBP was found to be associated with the separation of T-DOM from other AZ-DOM.

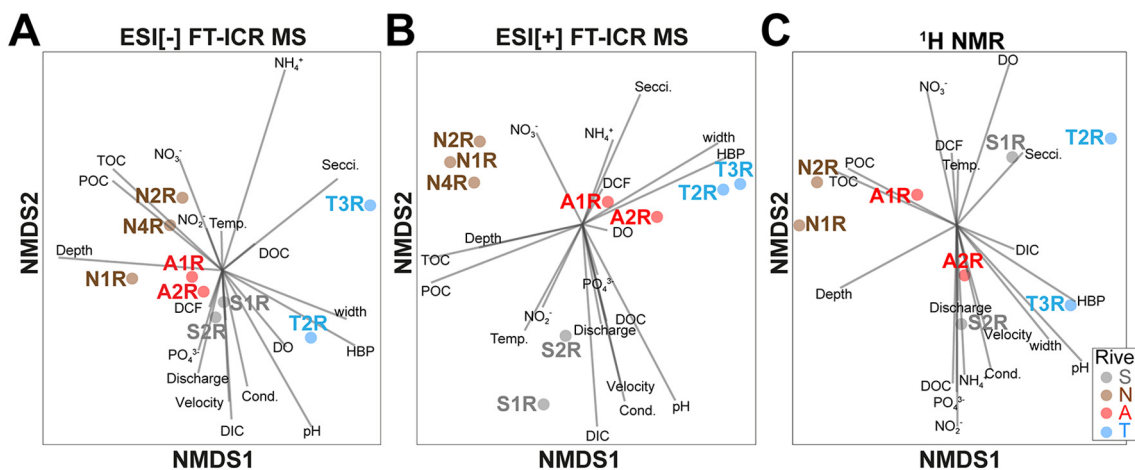


Fig. 5. NMDS analysis using DOM composition in the four Amazon main stem and tributaries based on A, B all assigned molecular formulae in ESI[±] FT-ICR MS, as well as C  $^1\text{H}$  NMR data at 0.01 ppm bucket resolution fitted with geochemical and biological data.

As DOC, POC, pH, and HBP showed more significant impacts on AZ-DOM composition in NMDS results (Tables S7-S8), we further tested their effects on ESI[±] FT-ICR MS-based molecular patterns by Spearman correlation analysis (Fig. S18). Higher POC was significantly correlated with higher abundance of polyphenolic CHO compounds and highly unsaturated CHNO compounds. In addition, pH showed positive correlation with compositions of smaller molecular weight ( $m/z$  200–400), less oxygenated CHO/CHNO and highly oxygenated CHNO/CHOS compounds. The molecular composition that correlated with lower pH included polyphenolic CHO compounds and highly unsaturated oxygen-rich CHO/CHNO compounds, which have potential to inhibit microbial decomposition (Freeman et al., 2001). Moreover, HBP was positively correlated with more oxygen-poor compounds of lower molecular weight (Fig. S18).

#### 4. Discussion

Solid phase extraction (SPE) with PPL resin (Dittmar et al., 2008) isolates the highest diversity of functionalized small organic molecules from freshwater and marine DOM with appreciable yield (Li et al., 2017). SPE of polydisperse and molecularly heterogeneous aqueous DOM is a dynamic process of sorption, desorption and resorption of individual molecules propagating through the PPL column (Li et al., 2016). We have followed strict guidelines during SPE with PPL resin (Li et al., 2016) and regard ecosystem characteristics of actual DOM molecules as well represented in our samples; slight variance of SPE selectivity may induce very minor but not relevant additional distinction.

Our joint molecular characterization of SPE-DOM in the Amazon main stem and tributaries by ESI[±] FT-ICR MS and  $^1\text{H}$  NMR provided improved resolution of the alterations of DOM along the Amazon River, and demonstrated distinct reactivity for CHO, CHNO, and CHOS molecules. The molecular features of AZ-DOM can serve as biogeochemical tracers and provide compelling information on their source, reactivity, and processing.

A group of more saturated CHO compounds was unique to T-DOM, likely resulting from abundant algal biomass and higher primary production in Tapajós (Moreira-Turcq et al., 2003a), in line with previous work that had in situ primary production of C4 grasses or algal material identified as the key autochthonous source of DOM in Tapajós River (Quay et al., 1992; Ward et al., 2016). Membrane lipids are known products of microbial degradation of phytoplankton and might serve as potential precursors of DOM (Harvey et al., 2006). Phytoplankton blooms provide new molecules relevant to the DOM pool in Amazon plume waters (Medeiros et al., 2015). Several studies have found very low chlorophyll *a* values in the white water rivers and high chlorophyll *a* in clear waters (Gagne-Maynard et al., 2017; Abril et al., 2014).

High abundance of highly oxygenated and highly unsaturated CHNO compounds, which ionized in both ESI[±] FT-ICR MS was observed in all the S/N/A/T-DOM. Detection of CHNO molecules differs in ESI[-] and ESI[+] MS methods because the former primarily ionizes carboxyl-carrying DOM molecules (like e.g. CRAM, carboxyl-rich alicyclic molecules (Hertkorn et al., 2006)), which are abundant in common freshwater DOM as observed e.g. by  $^{13}\text{C}$  NMR spectra and titration (Ritchie and Perdue, 2003). ESI[+] directly detects nitrogen containing molecules which not necessarily carry carboxylic groups. The complementary of “active” detection of N-containing molecules by ESI[+] and “passive” observation in ESI[-] MS allows compositional and structural distinction related to origin and processing of DOM. Hence, CHNO molecular compositions observed in both ESI[±] might originate from different (distributions of) isomers of identical compositions, with some probable emphasis on more recalcitrant nitrogen-containing CRAM. Moreover, the abundance of less oxygenated CHNO compounds that mostly ionized in ESI[+] FT-ICR MS was highest in AM1R and then declined rapidly; these more aliphatic compounds likely had a shorter residence time, in agreement with higher general biogeochemical processing of heteroatom-containing molecules (Ksionzek et al., 2016).

The higher content of S-containing compounds in S-DOM and AM1R may have resulted from incorporation of sulfur into organic matter by dissimilatory sulfate-reducing bacteria and/or by abiotic sulfurization reactions under anoxic conditions in sediment-rich waters like Solimões and Madeira (Luek et al., 2017; Sinninghe Damste and De Leeuw, 1990; Schmidt et al., 2009), but anthropogenic sources cannot be excluded (Latrubesse et al., 2017). Furthermore, DOM sulfurization processes are likely to be more intense under more anaerobic conditions during low-water periods relative to the high-water period we sampled.

Unlike mass spectrometry, which has intrinsic limitations like structure-dependent ionization efficiency (Hertkorn et al., 2008),  $^1\text{H}$  NMR more comprehensively covered all structures containing non-exchangeable hydrogen atoms, although the huge diversity of hydrogen atomic environments in DOM produced a considerable overlap of NMR resonances. N-DOM showed a higher degree of oxygenation relative to S/A/T-DOM in a very extensive range of aliphatic and aromatic carbon chemical environments. These molecular features were transferred to the Amazon River and became strongly attenuated ~150 km downstream. Moreover, A-DOM downstream of the Madeira River inflow and the Uatumã River inflow showed higher relative abundance of pure and functionalized aliphatic protons compared to A-DOM just upstream of these confluences, presumably indicative of higher proportions of more microbially processed terrestrial DOM (Lechtenfeld et al., 2015; Schmidt et al., 2009).

Solimões-Negro confluence ranks among the largest on Earth and provides non-conservative mixing and exemplary spatial and temporal DOM

processing on grand-scale. High DOC with large proportion of hydroxyl and phenolic sites in Negro water (Duarte et al., 2016; Gonsior et al., 2016) and abundant sediment load in Solimões water (Aucour et al., 2003; Moreira-Turcq et al., 2003b; Subdiaga et al., 2019) present favorable conditions for structure-selective sorption of OM on mineral surfaces (Aufdenkampe et al., 2001; Moreira-Turcq et al., 2003b; Subdiaga et al., 2019). Large proportions of polyphenolic compounds in N-DOM were removed from the DOM pool when Negro met Solimões. Many molecular formulae with near average H/C and O/C ratios prevailed in the Amazon River downstream, representing a large number of isomeric molecules that as a whole were resistant to rapid alteration. Continual lateral input of processed terrestrial and autochthonous organic matter from tributaries and floodplains probably contributed to this dynamic equilibrium of DOM synthesis and degradation.

Considerable decrease of DO (~30 %) and POC (~90 %) concentrations and concomitant increase of HBP and DCF just downstream of Solimões-Negro confluence reflected high microbial activity following mixing, as previously reported for mixing zones in the Amazon basin (Farjalla, 2014). The large depletion of POC at Solimões-Negro mixing zone, in addition to the large number of molecular signatures associated with POC in the Amazon River downstream (Fig. S18) suggest that the DOC-POC transition may have significant effects on DOM composition, especially at confluences. The POC/DOC concentration ratios were ~2 upstream of the Solimões-Negro mixing zone (both Negro and Solimões), while the ratios were ~0.2 downstream of Solimões-Negro mixing zone (Amazon). The loss of POC was probably associated with sedimentation processes, structure selective sorption of DOM molecules to minerals (Subdiaga et al., 2019), favored by a decrease in water velocity and an increase in the depth, as well as OM degradation (Moreira-Turcq et al., 2003b).

However, changes in AZ-DOM composition not only resulted from abiotic processes but were likely associated with considerable bacterial activity, as proved by high HBP rates. Previous studies suggested overall low aquatic bacterial metabolism for the Amazon waters, but confluences could be hot spot areas of high bacterial metabolism, which are associated with changes in organic matter quality (Farjalla, 2014). The less oxygenated, lower molecular weight CHO/CHNO compounds associated with higher HBP might be preferentially assimilated and converted into new bacterial biomass. Furthermore, we found for the first time that DCF contributed to microbial biomass production to the same or even higher extent than heterotrophic processes just downstream of the Solimões-Negro mixing zone, suggesting that the inorganic carbon pathway may be as important as organic carbon degradation when river waters with distinct characteristics converge. In addition, abiotic reactions such as photochemical processing (oxidation and mineralization) and metal complexation could also have important impact on changes of DOM composition in the Amazon River (Amon and Benner, 1996; Aucour et al., 2003).

The inherent complexity of DOM requires multiple analytical dimensions to understand its molecular processing within the carbon cycle. DOM analysis has been conducted by ESI[−] FT-ICR MS with certain preference for selective ionization of polar acidic functional groups (e.g., carboxylic acids), but poor propensity to ionize CHNO compounds lacking carboxyl and/or hydroxyl groups. Moreover, CHNO molecules represent important potentially biolabile components of DOM that indicate land cover, microbial processing, and possibly abiotic nitrogen incorporation (Bernhardt and Likens, 2002; Sleighter et al., 2014). The use of both negative and positive ESI modes for DOM research is highly complementary and beneficial, especially for DOM containing higher proportions of N-containing compounds resulting from higher microbial activity, such as in river confluences, highly autochthonous samples, permafrost thaw, and anthropogenically impacted streams (Spencer et al., 2019; Wagner et al., 2015). Furthermore, high-field proton NMR spectra, despite limited resolution because of massive intrinsic averaging, provided highly complementary quantitative DOM structural information, and enabled clear classification of AZ-DOM. Oxygenated SPE-DOM molecules were more efficiently ionized in ESI[−] FT-ICR MS, unsaturated and nitrogen-containing compounds were better ionized in ESI[+] FT-ICR MS, whereas 1D NMR showed better coverage of purely aliphatic structures not resolvable in mass spectra.

## 5. Conclusion

Complementary ESI[±] mass spectrometry and NMR spectroscopy provided comprehensive coverage of molecular evolution of DOM for exemplary processes in the Amazon basin, and distinct reactivity for CHO, CHNO and CHOS molecules.

So far elusive structural features of CHNO compounds in Amazon DOM, and DOM in other ecosystems/biomes, will become better constrained by comparative analysis of CHO and CHNO compounds in ESI[+] and ESI[−] mass spectra for individual samples and processes.

Joint ESI[±] mass spectrometry should become commonplace for further studies of DOM processing in ecosystems because strong ionization selectivity in ESI[−] mass spectra provides conceptual assessments with serious intrinsic limitations. NMR spectra offer valuable constraints of hydrogen and carbon atomic environments not available by FT mass spectra and are important for providing structural information and obtaining credible conclusions.

## CRediT authorship contribution statement

DB, AEP, MG, PS and NH designed research. JV, FMS, MH, DB, PS, MG, AEP, and NH participated in sampling. SL, JV, MH and NH prepared samples. SL and MH acquired FT-ICR MS spectra. SL and NH acquired NMR spectra. AEP, DB, and NH obtained funding. Data interpretation was performed by all authors. SL, NH, and MH actively participated in writing the manuscript. All authors provided significant contributions to the final manuscript.

## Data availability

Data will be made available on request.

## Declaration of competing interest

The authors declare that they have no known competing financial interests or personal relationships that could have appeared to influence the work reported in this paper.

## Acknowledgments

This work was supported by the Alexander von Humboldt Foundation (NH and AEP; Research Linkage Program: Connecting the diversity of DOM and CO<sub>2</sub> and CH<sub>4</sub> production in tropical lakes); the Swedish Research Council for Sustainable Development, FORMAS, grants no. 2013-01077 and 2021-0242, the Swedish Research Council (VR; grant no. 2012-00048), the European Research Council ERC (DB; grant no. 725546), the China Scholarship Council (LS; grant no. 201806360268) Molecular Level Characterization of Natural Organic Matter in Tropical Freshwater and Marine Ecosystems of Worldwide Relevance: Amazon Basin, Pantanal, Red Sea, and several grants from Brazilian Foundations CAPES (Probal), FAPERJ (Cientista do Nosso Estado) and CNPq (Universal and Ciencias sem Fronteiras) to AEP.

## Appendix A. Supplementary data

Supplementary data associated with this article can be found in the online version, at <https://doi.org/10.1016/j.scitotenv.2022.159620>. These data include the Google map of the most important areas described in this article.

## References

- Abril, G., Martinez, J.M., Artigas, L.F., Moreira-Turcq, P., Benedetti, M.F., Vidal, L., Meziane, T., Kim, J.H., Bernardes, M.C., Savoye, N., Deborde, J., Souza, E.L., Alberici, P., Landim de Souza, M.F., Roland, F., 2014. Amazon River carbon dioxide outgassing fuelled by wetlands. *Nature* 505 (7483), 395–398.

- Amado, A.M., Farjalla, V.F., Esteves Fde, A., Bozelli, R.L., Roland, F., Enrich-Prast, A., 2006. Complementary pathways of dissolved organic carbon removal pathways in clear-water Amazonian ecosystems: photochemical degradation and bacterial uptake. *FEMS Microbiol. Ecol.* 56 (1), 8–17.
- Amon, R.M.W., Benner, R., 1996. Photochemical and microbial consumption of dissolved organic carbon and dissolved oxygen in the Amazon River system. *Geochim. Cosmochim. Acta* 60 (10), 1783–1792.
- Armanious, A., Aepli, M., Sander, M., 2014. Dissolved organic matter adsorption to model surfaces: adlayer formation, properties, and dynamics at the nanoscale. *Environ. Sci. Technol.* 48 (16), 9420–9429.
- Aucour, A.M., Tao, F.X., Moreira-Turcq, P., Seyler, P., Sheppard, S., Benedetti, M.F., 2003. The Amazon River: behaviour of metals (Fe, Al, Mn) and dissolved organic matter in the initial mixing at the Rio Negro/Solimões confluence. *Chem. Geol.* 197 (1–4), 271–285.
- Aufdenkampe, A.K., Hedges, J.I., Richey, J.E., Krusche, A.V., Llerena, C.A., 2001. Sorptive fractionation of dissolved organic nitrogen and amino acids onto fine sediments within the Amazon Basin. *Limnol. Oceanogr.* 46 (8), 1921–1935.
- Bae, E., Yeo, I.J., Jeong, B., Shin, Y., Shin, K.H., Kim, S., 2011. Study of double bond equivalents and the numbers of carbon and oxygen atom distribution of dissolved organic matter with negative-mode FT-ICR MS. *Anal. Chem.* 83 (11), 4193–4199.
- Battin, T.J., Luysaert, S., Kaplan, L.A., Aufdenkampe, A.K., Richter, A., Tranvik, L.J., 2009. The boundless carbon cycle. *Nat. Geosci.* 2 (9), 598–600.
- Benner, R., Opsahl, S., Chin-Leo, G., Richey, J.E., Forsberg, B.R., 1995. Bacterial carbon metabolism in the Amazon River system. *Limnol. Oceanogr.* 40 (7), 1262–1270.
- Bernhardt, E.S., Likens, G.E., 2002. Dissolved organic carbon enrichment alters nitrogen dynamics in a forest stream. *Ecology* 83 (6), 1689–1700.
- Bianchi, T.S., Ward, N.D., 2019. Editorial: the role of priming in terrestrial and aquatic ecosystems. *Front. Earth Sci.* 7, 321.
- Cole, J.J., Prairie, Y.T., Caraco, N.F., McDowell, W.H., Tranvik, L.J., Striegl, R.G., Duarte, C.M., Kortelainen, P., Downing, J.A., Middelburg, J.J., Melack, J., 2007. Plumbing the global carbon cycle: integrating inland waters into the terrestrial carbon budget. *Ecosystems* 10 (1), 172–185.
- Dittmar, T., Koch, B., Hertkorn, N., Kattner, G., 2008. A simple and efficient method for the solid-phase extraction of dissolved organic matter (SPE-DOM) from seawater. *Limnol. Oceanogr. Methods* 6 (6), 230–235.
- do Nascimento, D.R., Sawakuchi, A.O., Guedes, C.C.F., Giannini, P.C.F., Grohmann, C.H., Ferreira, M.P., 2015. Provenance of sands from the confluence of the Amazon and Madeira rivers based on detrital heavy minerals and luminescence of quartz and feldspar. *Sediment. Geol.* 316, 1–12.
- Drake, T.W., Hemingway, J.D., Kurek, M.R., Peucker-Ehrenbrink, B., Brown, K.A., Holmes, R.M., Galy, V., Moura, J.M.S., Mitsuya, M., Wassenaar, L.I., Six, J., Spencer, R.G.M., 2021. The pulse of the Amazon: fluxes of dissolved organic carbon, nutrients, and ions from the world's largest river. *Glob. Biogeochem. Cycles* 35 (4), e2020GB006895.
- Duarte, R.M., Smith, D.S., Val, A.L., Wood, C.M., 2016. Dissolved organic carbon from the upper Rio Negro protects zebrafish (Danio rerio) against ionoregulatory disturbances caused by low pH exposure. *Sci. Rep.* 6 (1), 20377.
- Ertel, J.R., Hedges, J.I., Devol, A.H., Richey, J.E., Ribeiro, M.d.N.G., 1986. Dissolved humic substances of the Amazon River system I. *Limnol. Oceanogr.* 31 (4), 739–754.
- Farjalla, V.F., 2014. Are the mixing zones between aquatic ecosystems hot spots of bacterial production in the Amazon River system? *Hydrobiologia* 728 (1), 153–165.
- Freeman, C., Ostle, N., Kang, H., 2001. An enzymic 'latch' on a global carbon store. *Nature* 409 (6817), 149.
- Gagne-Maynard, W.C., Ward, N.D., Keil, R.G., Sawakuchi, H.O., Da Cunha, A.C., Neu, V., Brito, D.C., Da Silva Less, D.F., Diniz, J.E.M., De Matos Valerio, A., Kampel, M., Krusche, A.V., Richey, J.E., 2017. Evaluation of primary production in the lower Amazon River based on a dissolved oxygen stable isotopic mass balance. *Front. Mar. Sci.* 4, 1–12.
- Gonsior, M., Valle, J., Schmitt-Kopplin, P., Hertkorn, N., Bastviken, D., Luek, J., Harir, M., Bastos, W., Enrich-Prast, A., 2016. Chemodiversity of dissolved organic matter in the Amazon Basin. *Biogeosciences* 13 (14), 4279–4290.
- Harvey, H.R., Dyda, R.Y., Kirchman, D.L., 2006. Impact of DOM composition on bacterial lipids and community structure in estuaries. *Aquat. Microb. Ecol.* 42 (2), 105–117.
- Hedges, J.I., Ertel, J.R., Quay, P.D., Grootes, P.M., Richey, J.E., Devol, A.H., Farwell, G.W., Schmidt, F.W., Salati, E., 1986. Organic carbon-14 in the Amazon river system. *Science* 231 (4742), 1129–1131.
- Hedges, J.I., Hatcher, P.G., Ertel, J.R., Meyers-Schulte, K.J., 1992. A comparison of dissolved humic substances from seawater with Amazon River counterparts by <sup>13</sup>C-NMR spectrometry. *Geochim. Cosmochim. Acta* 56 (4), 1753–1757.
- Hedges, J.I., Cowie, G.L., Richey, J.E., Quay, P.D., Benner, R., Strom, M., Forsberg, B.R., 1994. Origins and processing of organic matter in the Amazon River as indicated by carbohydrates and amino acids. *Limnol. Oceanogr.* 39 (4), 743–761.
- Hertkorn, N., Benner, R., Frommberger, M., Schmitt-Kopplin, P., Witt, M., Kaiser, K., Ketttrup, A., Hedges, J.I., 2006. Characterization of a major refractory component of marine dissolved organic matter. *Geochim. Cosmochim. Acta* 70 (12), 2990–3010.
- Hertkorn, N., Ruecker, C., Meringer, M., Gugisch, R., Frommberger, M., Perdue, E.M., Witt, M., Schmitt-Kopplin, P., 2007. High-precision frequency measurements: indispensable tools at the core of the molecular-level analysis of complex systems. *Anal. Bioanal. Chem.* 389 (5), 1311–1327.
- Hertkorn, N., Frommberger, M., Witt, M., Koch, B.P., Schmitt-Kopplin, P., Perdue, E.M., 2008. Natural organic matter and the event horizon of mass spectrometry. *Anal. Chem.* 80 (23), 8908–8919.
- Hertkorn, N., Harir, M., Koch, B.P., Michalke, B., Schmitt-Kopplin, P., 2013. High-field NMR spectroscopy and FTICR mass spectrometry: powerful discovery tools for the molecular level characterization of marine dissolved organic matter. *Biogeosciences* 10 (3), 1583–1624.
- Hertkorn, N., Harir, M., Cawley, K.M., Schmitt-Kopplin, P., Jaffé, R., 2016. Molecular characterization of dissolved organic matter from subtropical wetlands: a comparative study through the analysis of optical properties, NMR and FTICR/MS. *Biogeosciences* 13 (8), 2257–2277.
- Kamjunke, N., Herzsprung, P., Neu, T.R., 2015. Quality of dissolved organic matter affects planktonic but not biofilm bacterial production in streams. *Sci. Total Environ.* 506–507, 353–360.
- Koch, B.P., Dittmar, T., 2006. From mass to structure: an aromaticity index for high-resolution mass data of natural organic matter. *Rapid Commun. Mass Spectrom.* 20 (5), 926–932.
- Ksionzek, K.B., Lechtenfeld, O.J., McCallister, S.L., Schmitt-Kopplin, P., Geuer, J.K., Geibert, W., Koch, B.P., 2016. Dissolved organic sulfur in the ocean: biogeochemistry of a petagram inventory. *Science* 354 (6311), 456–459.
- Latrubesse, E.M., Arima, E.Y., Dunne, T., Park, E., Baker, V.R., d'Horta, F.M., Wight, C., Wittmann, F., Zuanon, J., Baker, P.A., Ribas, C.C., Norgaard, R.B., Filizola, N., Ansar, A., Flyvbjerg, B., Stevaux, J.C., 2017. Damming the rivers of the Amazon basin. *Nature* 546 (7658), 363–369.
- Lechtenfeld, O.J., Hertkorn, N., Shen, Y., Witt, M., Benner, R., 2015. Marine sequestration of carbon in bacterial metabolites. *Nat. Commun.* 6 (1), 6711.
- Li, Y., Harir, M., Lucio, M., Kanawati, B., Smirnov, K., Flerus, R., Koch, B.P., Schmitt-Kopplin, P., Hertkorn, N., 2016. Proposed guidelines for solid phase extraction of Suwannee river dissolved organic matter. *Anal. Chem.* 88 (13), 6680–6688.
- Li, Y., Harir, M., Uhl, J., Kanawati, B., Lucio, M., Smirnov, K.S., Koch, B.P., Schmitt-Kopplin, P., Hertkorn, N., 2017. How representative are dissolved organic matter (DOM) extracts? A comprehensive study of sorbent selectivity for DOM isolation. *Water Res.* 116 (2017), 316–323.
- Luek, J.L., Thompson, K.E., Larsen, R.K., Heyes, A., Gonsior, M., 2017. Sulfate reduction in sediments produces high levels of chromophoric dissolved organic matter. *Sci. Rep.* 7 (1), 8829.
- Lynch, L.M., Sutfin, N.A., Fegel, T.S., Boot, C.M., Covino, T.P., Wallenstein, M.D., 2019. River channel connectivity shifts metabolite composition and dissolved organic matter chemistry. *Nat. Commun.* 10 (1), 459.
- Martinez, J.-M., Espinoza-Villar, R., Armijos, E., Silva Moreira, L., 2015. The optical properties of river and floodplain waters in the Amazon River Basin: implications for satellite-based measurements of suspended particulate matter. *J. Geophys. Res.* 120 (7), 1274–1287.
- Mayorga, E., Aufdenkampe, A.K., Masiello, C.A., Krusche, A.V., Hedges, J.I., Quay, P.D., Richey, J.E., Brown, T.A., 2005. Young organic matter as a source of carbon dioxide outgassing from Amazonian rivers. *Nature* 436 (7050), 538–541.
- McClain, M.E., Naiman, R.J., 2008. Andean influences on the biogeochemistry and ecology of the Amazon River. *Bioscience* 58 (4), 325–338.
- Medeiros, P.M., Seidel, M., Ward, N.D., Carpenter, E.J., Gomes, H.R., Niggemann, J., Krusche, A.V., Richey, J.E., Yager, P.L., Dittmar, T., 2015. Fate of the Amazon River dissolved organic matter in the tropical Atlantic Ocean. *Glob. Biogeochem. Cycles* 29 (5), 677–690.
- Moreira-Turcq, P., Seyler, P., Guyot, J.L., Etcheber, H., 2003a. Exportation of organic carbon from the Amazon River and its main tributaries. *Hydrol. Process.* 17 (7), 1329–1344.
- Moreira-Turcq, P.F., Seyler, P., Guyot, J.L., Etcheber, H., 2003b. Characteristics of organic matter in the mixing zone of the Rio Negro and Rio Solimões of the Amazon River. *Hydrol. Process.* 17 (7), 1393–1404.
- Mortillaro, J.M., Abril, G., Moreira-Turcq, P., Sobrinho, R.L., Perez, M., Meziane, T., 2011. Fatty acid and stable isotope ( $\delta^{13}C$ ,  $\delta^{15}N$ ) signatures of particulate organic matter in the lower Amazon River: seasonal contrasts and connectivity between floodplain lakes and the mainstem. *Org. Geochem.* 42 (10), 1159–1168.
- Pérez, M.A.P., Moreira-Turcq, P., Gallard, H., Allard, T., Benedetti, M.F., 2011. Dissolved organic matter dynamic in the Amazon basin: sorption by mineral surfaces. *Chem. Geol.* 286 (3–4), 158–168.
- Powers, L.C., Hertkorn, N., McDonald, N., Schmitt-Kopplin, P., Del Vecchio, R., Blough, N.V., Gonsior, M., 2019. Sargassum sp. act as a large regional source of marine dissolved organic carbon and polyphenols. *Glob. Biogeochem. Cycles* 33 (11), 1423–1439.
- Quay, P.D., Wilbur, D., Richey, J.E., Hedges, J.I., Devol, A.H., Victoria, R., 1992. Carbon cycling in the Amazon River: implications from the <sup>13</sup>C compositions of particles and solutes. *Limnol. Oceanogr.* 37 (4), 857–871.
- Quay, P.D., Wilbur, D., Richey, J.E., Devol, A.H., Benner, R., Forsberg, B.R., 1995. The 18O:16O of dissolved oxygen in rivers and lakes in the Amazon Basin: determining the ratio of respiration to photosynthesis rates in freshwaters. *Limnol. Oceanogr.* 40 (4), 718–729.
- Richey, J.E., Melack, J.M., Aufdenkampe, A.K., Ballester, V.M., Hess, L.L., 2002. Outgassing from Amazonian rivers and wetlands as a large tropical source of atmospheric CO<sub>2</sub>. *Nature* 416 (6881), 617–620.
- Ritchie, J.D., Perdue, E.M., 2003. Proton-binding study of standard and reference fulvic acids, humic acids, and natural organic matter. *Geochim. Cosmochim. Acta* 67 (1), 85–96.
- Saliot, A., Mejanelle, L., Scribe, P., Fillaux, J., Pepe, C., Jabaud, A., Dagaut, J., 2001. Particulate organic carbon, sterols, fatty acids and pigments in the Amazon River system. *Biogeochemistry* 53 (1), 79–103.
- Santoro, A.L., Bastviken, D., Gudas, C., Tranvik, L., Enrich-Prast, A., 2013. Dark carbon fixation: an important process in lake sediments. *PLoS One* 8 (6), e65813.
- Santos-Junior, C.D., Sarmento, H., de Miranda, F.P., Henrique-Silva, F., Logares, R., 2020. Uncovering the genomic potential of the Amazon River microbiome to degrade rainforest organic matter. *Microbiome* 8 (1), 151.
- Schmidt, F., Elvert, M., Koch, B.P., Witt, M., Hinrichs, K.-U., 2009. Molecular characterization of dissolved organic matter in pore water of continental shelf sediments. *Geochim. Cosmochim. Acta* 73 (11), 3337–3358.
- Seidel, M., Yager, P.L., Ward, N.D., Carpenter, E.J., Gomes, H.R., Krusche, A.V., Richey, J.E., Dittmar, T., Medeiros, P.M., 2015. Molecular-level changes of dissolved organic matter along the Amazon River-to-ocean continuum. *Mar. Chem.* 177, 218–231.
- Seidel, M., Dittmar, T., Ward, N.D., Krusche, A.V., Richey, J.E., Yager, P.L., Medeiros, P.M., 2016. Seasonal and spatial variability of dissolved organic matter composition in the lower Amazon River. *Biogeochemistry* 131 (3), 281–302.
- Shen, Y.-H., 1999. Sorption of natural dissolved organic matter on soil. *Chemosphere* 38 (7), 1505–1515.
- Simpson, A.J., McNally, D.J., Simpson, M.J., 2011. NMR spectroscopy in environmental research: from molecular interactions to global processes. *Prog. Nucl. Magn. Reson. Spectrosc.* 58 (3–4), 97–175.

- Sinninghe Damste, J.S., De Leeuw, J.W., 1990. Analysis, structure and geochemical significance of organically-bound sulphur in the geosphere: state of the art and future research. *Org. Geochem.* 16 (4–6), 1077–1101.
- Sleighter, R.L., Chin, Y.-P., Arnold, W.A., Hatcher, P.G., McCabe, A.J., McAdams, B.C., Wallace, G.C., 2014. Evidence of incorporation of abiotic S and N into prairie wetland dissolved organic matter. *Environ. Sci. Technol. Lett.* 1 (9), 345–350.
- Spencer, R.G., Kellerman, A.M., Podgorski, D.C., Macedo, M.N., Jankowski, K., Nunes, D., Neill, C., 2019. Identifying the molecular signatures of agricultural expansion in Amazonian headwater streams. *J. Geophys. Res. Biogeosci.* 124 (6), 1637–1650.
- Subdiaga, E., Orsetti, S., Haderlein, S.B., 2019. Effects of sorption on redox properties of natural organic matter. *Environ. Sci. Technol.* 53 (24), 14319–14328.
- Tziotis, D., Hertkorn, N., Schmitt-Kopplin, P., 2011. Kendrick-analogous network visualisation of ion cyclotron resonance Fourier transform mass spectra: improved options for the assignment of elemental compositions and the classification of organic molecular complexity. *Eur. J. Mass Spectrom. (Chichester)* 17 (4), 415–421.
- Wagner, S., Riedel, T., Niggemann, J., Vähätalo, A.V., Dittmar, T., Jaffé, R., 2015. Linking the molecular signature of heteroatomic dissolved organic matter to watershed characteristics in world rivers. *Environ. Sci. Technol.* 49 (23), 13798–13806.
- Ward, N.D., Bianchi, T.S., Sawakuchi, H.O., Gagne-Maynard, W., Cunha, A.C., Brito, D.C., Neu, V., de Matos Valerio, A., da Silva, R., Krusche, A.V., Richey, J.E., Keil, R.G., 2016. The reactivity of plant-derived organic matter and the potential importance of priming effects along the lower Amazon River. *J. Geophys. Res. Biogeosci.* 121 (6), 1522–1539.